RSC Advances

PAPER

View Article Online
View Journal | View Issue

Cite this: *RSC Adv.*, 2017, **7**, 2804

Theoretical investigation on the balance between large band gap and strong SHG response in BMO_4 (M = P and As) crystals†

Yanzhou Sun, Zhihua Yang,* Dianwei Hou and Shilie Pan*

Received 9th November 2016
Accepted 1st December 2016

DOI: 10.1039/c6ra26568e

www.rsc.org/advances

Nonlinear optical (NLO) materials with outstanding performances are particularly important in laser science. To design an efficient NLO material with an optimal balance between the optical band gap and the NLO coefficient is still a huge challenge. In this paper, the electronic structures and optical properties of two isostructural non-centrosymmetric BMO_4 (M = P and As) crystals exclusively containing tetrahedral groups have been studied by the first-principles method. Our calculated results show the compounds exhibit excellent properties with a suitable balance of large band gap and large NLO coefficient for BPO_4 (10.4 eV and 0.64 pm V^{-1}) and $BAsO_4$ (7.8 eV and 1.58 pm V^{-1}). The unanticipated large second-harmonic generation (SHG) response can be understood by the relatively strong s–p hybridization in BMO_4 (M = P and As). It is found that substitution of PO_4 groups for AsO_4 groups can increase the SHG effect and the birefringence but decrease the band gap. Whether the redshift of bandgap will be responsible for the change of SHG effect between BMO_4 (M = P and As) is explored by energy correction method. The increased polarizability anisotropy of tetrahedral groups explained the enhanced birefringence.

Introduction

Nonlinear optical (NLO) crystals have attracted much attention because they can be used to extend the working wavelength range of a solid state laser through frequency conversion.[1,2] For ultraviolet (UV) or deep-UV NLO applications, ideal NLO materials require a strict combination of properties that need to be satisfied simultaneously in a non-centrosymmetric crystal: a wide transparency window down to the deep-UV region, relatively strong effective second-harmonic generation (SHG) response, and suitable birefringence to realize phase matching. Borate and phosphate crystals have attracted much interest for their excellent performance as NLO crystals, such as, KH_2PO_4 (KDP),[3] CsB_3O_5,[4] LiB_3O_5 (LBO),[5] SrB_4O_7,[6] $LiCs_2PO_4$,[7] $Ba_3P_3O_{10}Cl$,[8] $Ba_5P_6O_{20}$,[9] and $RbBa_2(PO_3)_5$.[10] The tetrahedral BO_4 or PO_4 groups existing in the above mentioned crystals enlarge the band gaps of the crystals shifting the cutoff edge to the deep-UV region. However, the crystals with BO_4 or PO_4 groups as building blocks are usually labeled by small NLO coefficients and/or small birefringence. The combination of the π-conjugated planar BO_3 groups into the structures is away to improve the birefringence and optical nonlinearities of these crystals.[11–16] Especially, $KBe_2BO_3F_2$ (KBBF) has a short deep-UV cutoff wavelength about 150 nm, a relatively large SHG tensor d_{11} about 0.47 pm V^{-1}, and a moderate birefringence of 0.077. And it is the sole NLO crystal, which can generate coherent light of wavelength below 200 nm by the direct SHG at room temperature.[17] However, KBBF crystal is very difficult to grow in thickness due to its strong layering growth habit, which severely hinders its practical applications.[18]

In 1934, the cristobalite like forms of the ternary silica analogues BPO_4 were first discovered by solid-state synthesis at high temperature.[19] The theoretical or experimental researches of BPO_4 on its growth and optical properties have been in progress for many years.[20–24] They measured BPO_4 has a NLO coefficient d_{36} = 0.76 pm V^{-1}, which is larger than that of KBBF (d_{11} = 0.47 pm V^{-1}). BPO_4 also has a short deep-UV cutoff wavelength ~134 nm, 16 nm shorter than that of KBBF.[24] BPO_4 should have a smaller NLO coefficient resulting from the larger band gap because the possibility of quantum transition between valence and conduction bands is ratio to the reciprocal of diverse energy at each momentum point. Until 2016, Li *et al.* explained the mechanism of its large NLO coefficient.[25] Unsatisfactorily, BPO_4 has a smaller birefringence (approximately 0.007) than KBBF, which makes it non-phase matched in ultraviolet SHG progress, limiting its application in ultraviolet output. Therefore, the issue of how to improve the birefringence of the available frequency conversion material should be focused on. Previous studies have promised strain engineering and ion-doping methods could modulate or even enhance the

Key Laboratory of Functional Materials and Devices for Special Environments of CAS, Xinjiang Key Laboratory of Electronic Information Materials and Devices, Xinjiang Technical Institute of Physics & Chemistry of CAS, 40-1 South Beijing Road, Urumqi 830011, China. E-mail: zhyang@ms.xjb.ac.cn

† Electronic supplementary information (ESI) available. See DOI: 10.1039/c6ra26568e

birefringence of relevant materials both theoretically and experimentally.[26–30] Following this idea, we "look away" to arsenic, which is similar to phosphorus can coordinate with four oxygen atoms to form the tetrahedral groups. Curiously, does the combination of the BO_4 and AsO_4 groups result in an optimal balance between large band gap and strong SHG response? Does the value of birefringence also increase compared to BPO_4? To the best of our knowledge, theoretical or experimental reports about the optical properties of $BAsO_4$ are still absent after it was discovered due to the difficulty in growth.[31–33]

In this paper, in order to explore the influence on optical properties by the substitution of NLO-active PO_4 groups for AsO_4 groups, BMO_4 (M = P and As) crystals exclusively containing tetrahedral groups are studied. We first introduced the optical properties obtained by *ab initio* method. Then, the gap-determination factor was discussed to explain the mechanism of large band gaps in BMO_4 (M = P and As) crystals. $BAsO_4$ has a stronger SHG response with 2.5 times than that of BPO_4. The origin and enhancement of the large SHG effect of $BAsO_4$ was explored by combining the band structures and the energy correction analysis. Finally, we systemically discussed the polarizability anisotropy of tetrahedral groups to explain why the birefringence of $BAsO_4$ is 2.6 times than that of BPO_4.

Calculation methods

The first-principles calculations for electronic structure employed the planewave pseudopotential method in the CASTEP.[34–36] The calculations was performed using the crystallographic information files BPO_4: ICSD-4132434; $BAsO_4$: ICSD-413438. During the calculation, geometry optimization was performed using the BFGS minimization technique. The converged criterions for the geometry optimization are that the residual forces on the atoms, the displacements of atoms and the energy change were less than, 5.0×10^{-6} eV per atom, 0.01 eV $Å^{-1}$ and 5×10^{-4} Å, respectively. Two exchange and correlation functionals, local density approximation/Ceperley–Alder–Perdew–Zunger (LDA/CA–PZ)[37,38] and generalized gradient approximation/Perdew–Burke–Ernzerhof (GGA/PBE)[39] were adopted to calculate the electronic structures and NLO coefficients. After a series of successful tests, the LDA/CA–PZ functional with ultrasoft pseudopotentials (USP)[40] was finally selected, giving the best agreement with the experimental data of BPO_4. The valence electrons were B-$2s^2 2p^1$, O-$2s^2 2p^4$, P-$3s^2 3p^3$ and As-$4s^2 4p^3$, respectively. The number of plane waves was determined by a cutoff energy of 380 eV and the k-point sampling was set as $7 \times 7 \times 8$.

Based on the electronic structures, the imaginary part of the dielectric constant $\varepsilon_2(\omega)$ can be obtained by

$$\varepsilon_2 = \frac{2e^2\pi}{\Omega\varepsilon_0} \sum k, \mathrm{v}, \mathrm{c} \left\langle \varphi_{\mathrm{c}}{}^{k} | u \cdot r | \varphi_{\mathrm{k}}^{\mathrm{v}} \right\rangle^2 \delta\left(E_{\mathrm{k}}^{\mathrm{c}} - E_{\mathrm{k}}^{\mathrm{c}} - E\right) \quad (1)$$

In which Ω is the volume of the elemental cell, v, and c represent the valence and conduction bands, respectively, and u is the vector defining the polarization of the electric field of the incident light. The real part of the dielectric constant, and then the refractive index n and birefringence $\Delta n = n_{\max} - n_{\min}$ can be obtained using the Kramers–Kronig transform.[41] It is well known that although the LDA functional always underestimates the bandgap, after the scissors corrections were employed, reliable refractive indices and birefringence can still be got from the LDA calculations.[42–45] To get suitable scissors corrections of these two compounds, the modified Becke–Johnson (mBJ) exchange potential[46,47] and implemented in WIEN2k[48] was used to calculate the optical band gap because the mBJ method can get similar accuracy comparison with very expensive GW calculations[49,50] and experimental values.[22] Besides above methods, PBE0 hybridization functional has also been utilized to estimate the bandgaps in this work.

In addition, Becke three-parameter Lee–Yang–Parr (B3LYP) exchange correlation functional with the Lee–Yang–Parr correlation functional at the 6-31G basis set in Gaussian 09W program[51] were employed to calculate the polarizability of the tetrahedra groups MO_4 (M = B, P and As). The anisotropic polarizabilities ($\Delta\alpha$) are defined by the following equation:

$$\Delta\alpha = (1/2)^{1/2}[(\alpha_{xx} - \alpha_{yy})^2 + (\alpha_{xx} - \alpha_{zz})^2 + (\alpha_{zz} - \alpha_{yy})^2]^{1/2} \quad (2)$$

SHG coefficients were calculated at a zero frequency limit by the length-gauge formalism derived by Aversa and Sipe,[52] and later developed by Zhang *et al.*[27]

$$\chi^{(2)}_{\alpha\beta\gamma} = \chi^{(2)}_{\alpha\beta\gamma}(\mathrm{VE}) + \chi^{(2)}_{\alpha\beta\gamma}(\mathrm{VH}) \quad (3)$$

where,

$$\chi^{(2)}_{\alpha\beta\gamma}(\mathrm{VH}) = \frac{e^3}{2\hbar^2 m^3} \sum_{\mathrm{vv'c}} \int \frac{d^3k}{4\pi^3} P(\alpha\beta\gamma) \mathrm{Im}\left[p_{\mathrm{vv'}}{}^{\alpha} p_{\mathrm{v'c}}{}^{\beta} p_{\mathrm{cv}}{}^{\gamma}\right] \times \left(\frac{1}{\omega_{\mathrm{cv}}{}^3 \omega_{\mathrm{v'c}}{}^2} + \frac{2}{\omega_{\mathrm{vc}}{}^4 \omega_{\mathrm{cv'}}}\right) \quad (4)$$

$$\chi^{(2)}_{\alpha\beta\gamma}(\mathrm{VE}) = \frac{e^3}{2\hbar^2 m^3} \sum_{\mathrm{vcc'}} \int \frac{d^3k}{4\pi^3} P(\alpha\beta\gamma) \mathrm{Im}\left[p_{\mathrm{vc}}{}^{\alpha} p_{\mathrm{cc'}}{}^{\beta} p_{\mathrm{c'v}}{}^{\gamma}\right] \times \left(\frac{1}{\omega_{\mathrm{cv}}{}^3 \omega_{\mathrm{vc'}}{}^2} + \frac{2}{\omega_{\mathrm{vc}}{}^4 \omega_{\mathrm{c'v}}}\right) \quad (5)$$

here, α, β, γ are Cartesian components, v and v′ denote valence bands, c and c′ denote conduction bands, and $P(\alpha\beta\gamma)$ denotes full permutation. The band energy difference and momentum matrix elements are denoted as ω_{ij} and $p_{ij}{}^{\alpha}$, respectively.

Results and discussion

Structure and optical properties

BPO_4 and $BAsO_4$ crystallize in the tetragonal space group $I\bar{4}$ (no. 82), with $a = b = 4.3401$ Å, $c = 6.6470$ Å, $Z = 2$ for BPO_4, $a = b = 4.4658$ Å, $c = 6.8139$ Å, $Z = 2$ for $BAsO_4$, respectively. As sketched in Fig. 1, a continuous 3D framework of BMO_4 (M = P and As) crystals is built by sharing the corner of the BO_4 and MO_4 (M = P, As) tetrahedra.

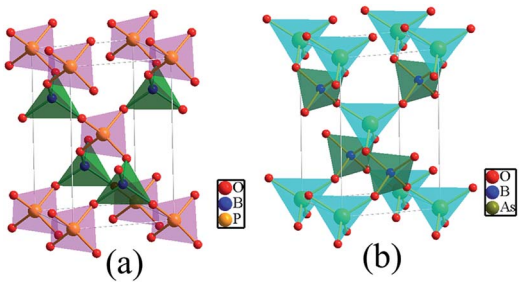

Fig. 1 The crystal structure of BPO_4 (a) and $BAsO_4$ (b).

Table 1 The optical properties of BMO_4 (M = P and As)

	Gap (eV)	SHG (pm V^{-1})	Δn
BPO_4	10.4	0.64	0.011
$BAsO_4$	7.8	1.58	0.029

The band gaps, SHG coefficients in static limit and the birefringences for BMO_4 (M = P and As) were obtained (shown in Table 1). As compared with the experimental results, the PBE0 functional gives reliable values that are estimated of 10.4 eV and 7.8 eV, respectively. It is well known that although the LDA and GGA functional always underestimates the bandgap, after the scissors corrections were employed, reliable SHG coefficient and birefringence can still be got from the LDA calculations. It is clearly shown that the largest calculated NLO coefficient d_{36} = 1.58 pm V^{-1} of $BAsO_4$ also is larger than that d_{36} = 0.64 pm V^{-1} of BPO_4, which is very closed to the experimentally measured value of about two times of KDP.[22] And the calculated birefringences are 0.011 for BPO_4, and 0.029 for $BAsO_4$ at 589 nm. The calculated birefringence about 0.011 is consistent well with the experimental value 0.007 at 589 nm.[24] It should be noticed that the band gap and NLO coefficient of $BAsO_4$ are comparable to these of the commercial NLO crystals LBO (7.8 eV and 1.17 pm V^{-1}), β-BaB_2O_4 (6.6 eV and 2.26 pm V^{-1}) and $KTiOPO_4$ (3.2 eV and 3.24 pm V^{-1}).[53] A subtle balance is obtained between large band gap and strong SHG response in $BAsO_4$ crystal. It indicates that $BAsO_4$ may have a promising potential to be a NLO material in UV or even DUV region.

Role of AsO_4 in band gap

LDA and GGA functionals are performed to calculate the band gap of BMO_4 (M = P and As), as shown in Table 2. The LDA and GGA results are smaller than the experimental data 9.25 eV (corresponding to the measured optical cutoff edge of 134 nm). It is not strange at all because the Kohn–Sham schemes based on LDA and GGA usually underestimate the band gap of materials primarily owning to the discontinuity of exchange–correlation energy. For comparison, the experimental optical bandgaps, the PBE0 and mBJ methods are also employed. It is found that PBE0 result is close to the experimental one. The results clearly indicate the validity of the method used here, so the optical bandgaps of BMO_4 (M = P and As) are very large

Table 2 Band gaps (eV) based on various exchange and correlation functionals

	BPO_4	$BAsO_4$
LDA	7.62	5.32
GGA	7.22	4.75
PBE0	10.35	7.77
mBJ	10.62	7.55
Exp.	9.25 (ref. 22)	—

(10.4 eV and 7.8 eV), comparable to the crystals aimed in deep-UV region such as $Ba_3P_3O_{10}Cl$ (6.9 eV),[8] $Li_4Sr(BO_3)_2$ (6.5 eV)[14] and KBBF (8.3 eV),[17] $NaSr_3Be_3B_3O_9F_4$ (7.2 eV)[54] and can be used in the UV region as NLO materials.

To explore the reason for the large band gaps, the partial density of states (PDOS) for BMO_4 (M = P and As) are plotted in Fig. 2a and b. For BPO_4, the upper of the valence band (VB) is mainly occupied by the non-bonding 2p orbitals of O; the bottom of the conduction band (CB) mainly consists of the hybridization orbitals of B–O and P–O. Similar to BPO_4, the contributions of O 2p orbitals primarily dominate the upper VB of $BAsO_4$. However, the bottom of CB of $BAsO_4$ mainly consists of As-s, B-p, O-p. To gain a deeper understanding of the electric structure features and check the band-gap determiner, we plotted slices of orbital density of CB minimum and VB maximum as shown in Fig. 2c–f. From Fig. 2c and e, it concludes that the VB maximum in BMO_4 (M = P and As) is

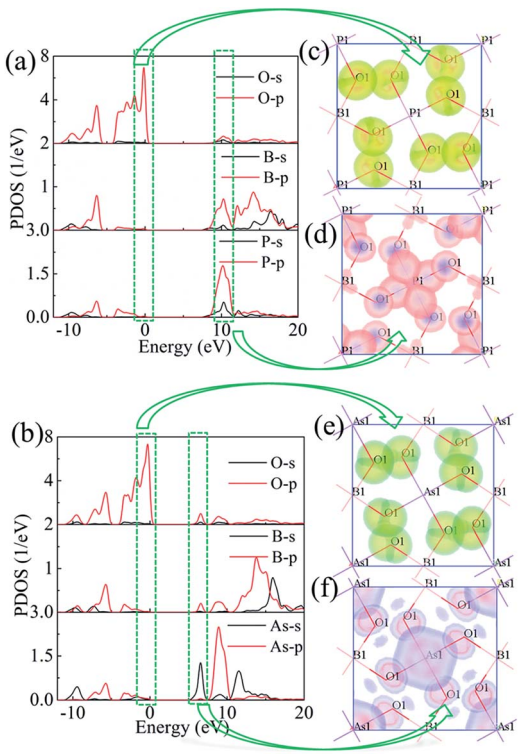

Fig. 2 The partial density of states (PDOS) for BPO_4 (a) and $BAsO_4$ (b). The energy range of the specific orbitals of the BPO_4 crystals (c), (d) and the $BAsO_4$ crystals (e), (f).

Table 3 HOMO and LUMO of MO_4 (M = B, P and As) groups and BO_3 groups

Units	HOMO (a.u.)	LUMO (a.u.)	Gap (a.u.)
BO_4	1.064	1.459	0.395
PO_4	0.443	0.775	0.332
AsO_4	0.424	0.729	0.305
BO_3	0.578	0.898	0.311

mainly occupied by the nonbonding oxygen orbitals. While CB minimum exhibits totally different characters for the title compounds. It is clearly shown that the orbitals from P atoms, O atoms and B atoms dominate VB maximum of BPO_4 (see Fig. 2d). However, for $BAsO_4$, the VB maximum is primarily only controlled by orbitals from As and O atoms without B atoms as shown in Fig. 2f. Therefore, one can make a conclusion that the band gap determiner is nonbonding 2p of O under Fermi level and hybridization orbitals of B/P–O in CB for BPO_4 crystal, and As–O in CB for $BAsO_4$ crystal. In addition, the orbital density also reveals a strong hybridization between As-s and O-p in Fig. 2e. Such strong sp hybridization in $BAsO_4$ leads to a slight red-shift of the deep-UV cutoff edge compared with BPO_4.

In the light of the frontier molecular orbitals theory, the HOMO (highest occupied molecular orbital) and LUMO (lowest unoccupied molecular orbital) of MO_4 (M = B, P and As) and BO_3 groups were also obtained (Table 3). Evidently, the band gaps ΔE_g of the MO_4 (M = B, P and As) tetrahedral groups and BO_3 groups obey the following relative orders: ΔE_g (BO_4) > ΔE_g (PO_4) > ΔE_g (AsO_4) ≈ ΔE_g (BO_3). It should pay attention to that the band gaps of AsO_4 groups is comparable with that of BO_3 groups revealing AsO_4 to be as a NLO active unit which is also beneficial to the large band gap.

Mechanism for strong and enhanced SHG response

SHG coefficients d_{ij} were estimated by the sum-over-states under the static limit within the length gauge.[27] BMO_4 (M = P and As) both belong to $I\bar{4}$ space group, owing to the restriction of Kleinman's symmetry, there are two independent elements: d_{36} and d_{15}. The calculated results are listed in Table 4. It is clearly shown that the largest SHG tensor for BPO_4 is $d_{36} = 0.64$ pm V^{-1} which is comparable to the reported value $d_{36} = 0.78$ pm V^{-1}.[22] As for $BAsO_4$, the SHG coefficients $d_{36} = 1.58$ pm V^{-1} and $d_{15} = 1.04$ pm V^{-1} are obtained, respectively.

As mentioned above, BMO_4 (M = P and As) should have a weaker NLO response resulting from the large band gap. Curiously, SHG response is 2 × KDP for BPO_4 and 4 × KDP for BAsO4, which is larger than many crystals with equivalent bang gap like KBBF (1.2 × KDP, 8.3 eV). To illuminate this question, we carefully check the band structures of BMO_4 (M = P and As) (shown in the Fig. 3). We mainly focused on the electric structure around the Fermi energy level because the optical properties of the crystal are particularly determined by the states close to the Fermi level. Evidently, the lowest conducting band is only dispersive around the G point (dyed by blue), and valence bands are clearly dispersive. It implies a relatively strong hybridization between the O 2p orbitals and the 4s orbitals from As which can enhance the interband Berry connection, and contribute a relatively large SHG effect in $BAsO_4$. The same situation (see the Fig. 3a) also occurs in the BPO_4 crystal.[25]

Table 4 The SHG response of two SHG tensors (pm V^{-1}) of BMO_4 (M = P and As)

Compound	d_{36}	d_{15}
BPO_4	0.64	−0.07
$BAsO_4$	−1.58	1.04

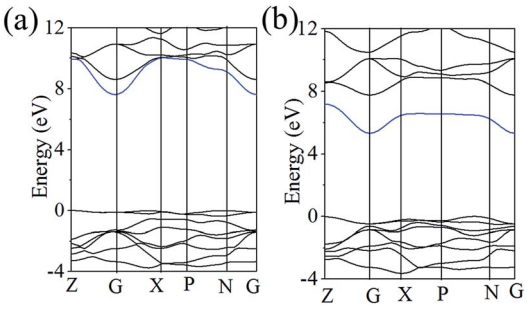

Fig. 3 The band structures of BPO_4 (a) and $BAsO_4$ (b).

To identify the contribution of each atom in the SHG processes in real space, the SHG-density method was analyzed for both compounds. The SHG process contains the two virtual transition processes, namely virtual electron (VE) and virtual hole (VH) processes. Here we will just show the SHG-density of the largest SHG tensors d_{36} to discuss the origin of the SHG effect. The obtained SHG-densities of the two compounds are shown in Fig. S1† and 4. More attention will be paid on that the SHG-density of BMO_4 (M = P and As) mainly distributes around the BO_4 and MO_4 groups (especially on O^{2-} anions) for unoccupied states and occupied states, illustrating their dominant contributions to the SHG.

It is worth to notice that $BAsO_4$ has SHG response about 2.5 × BPO4. Curiously what is the origin of the largely enhanced

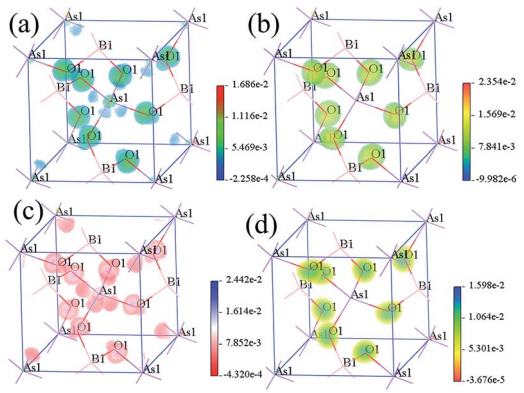

Fig. 4 SHG-density of $BAsO_4$: (a) VE occupied states; (b) VE unoccupied states; (c) VH occupied states; (d) VH unoccupied states.

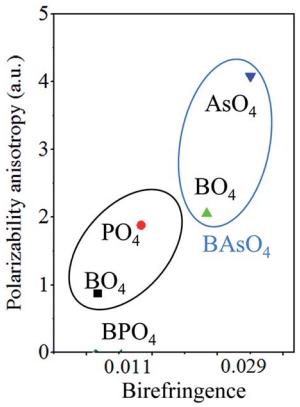

Fig. 5 Calculated polarizability anisotropy $\Delta\alpha$ of tetrahedral groups in BMO_4 (M = P and As).

SHG coefficients of $BAsO_4$? It is well known that band gap has a significant influence on SHG effect that the small gap can change the SHG response dramatically. To check the influence of the decrease of band gap in $BAsO_4$, we use the scissor operator corrections to the experimental band gaps of BPO_4. It turns out that the band-gap-corrected SHG coefficient d_{36} is 0.79 pm V^{-1} for $BAsO_4$, which is close to that of BPO_4 (d_{36} = 0.64 pm V^{-1}). Compared with 1.58 pm V^{-1}, we found that the contribution induced by band gap reduction is around 85%. And we know from the electronic structure that the band gap reduction or the red-shift of UV-cutoff from BPO_4 to $BAsO_4$ attributes to the strong hybridization interaction between As and O. Therefore, the stronger covalent interaction of As–O is a significant factor to the enhanced SHG response in $BAsO_4$ compared that of BPO_4.

Origin of enhanced birefringence

The obtained birefringence of $BAsO_4$ is about 2.6 × BPO_4. In order to figure out the enhancement, we calculate the polarizability anisotropy of BO_4, PO_4 and AsO_4 groups in BMO_4 (M = P and As) using the DFT implemented *via* the Gaussian09 package at the 6-31 G level. The polarizability anisotropy $\Delta\alpha$ of BO_4, PO_4 and AsO_4 groups are shown in the Fig. 5. It is clearly the $\Delta\alpha$ of tetrahedral groups of $BAsO_4$ are larger than those of BPO_4. The sequence of the calculated polarizability anisotropy is in good agreement with the sequence of birefringence.

Conclusion

In this paper, the electronic structures and optical properties of BMO_4 (M = P and As) were calculated by DFT method. The band gap of $BAsO_4$ is still large after a substitution of NLO active PO_4 groups for AsO_4 groups. The band gaps ΔE_g of the groups MO_4 (M = B, P and As) and BO_3 groups obey the following relative orders: ΔE_g (BO_4) > ΔE_g (PO_4) > ΔE_g (AsO_4) ≈ ΔE_g (BO_3). It implies AsO_4 groups to be as a NLO active unit which is also in favour of the large band gap. We also found BMO_4 (M = P, As) have large SHG responses. A relatively strong hybridization between the O 2p orbitals and the orbitals from B/P or As contributes a relatively large SHG effect in BMO_4 (M = P, As). The strong s–p hybridization influence between As and O gives the band gap reduction and the 85% enhancement of SHG response from BPO_4 to $BAsO_4$. The calculated birefringence of $BAsO_4$ is about 2.6 × BPO_4 due to the stronger polarizability anisotropy of tetrahedral groups in $BAsO_4$ than those of BPO_4. The results show the replacing PO_4 tetrahedra by AsO_4 groups do not only achieve an optimal balance between large band gap and strong SHG response but also are helpful to increase birefringence. And one may be able to design new compounds with the adjustment effect of tetrahedral groups.

Acknowledgements

This work is supported by the National Key Basic Research Program of China (Grant No. 2014CB648400), the "National Natural Science Foundation of China" (Grant No. 51425206, 11474353), the Xinjiang International Science & Technology Cooperation Program (20146001).

References

1 D. Cyranoski, *Nature*, 2009, **457**, 953–955.
2 P. Becker, *Adv. Mater.*, 1998, **10**, 979–992.
3 J. De Yoreo, A. Burnham and P. Whitman, *Int. Mater. Rev.*, 2002, **47**, 113–152.
4 Y. C. Wu, T. Sasaki, S. Nakai, A. Yokotani, H. G. Tang and C. T. Chen, *Appl. Phys. Lett.*, 1993, **62**, 2614–2615.
5 C. T. Chen, Y. C. Wu, A. D. Jiang, B. C. Wu, G. M. You, R. K. Li and S. J. Lin, *J. Opt. Soc. Am. B*, 1989, **6**, 616–621.
6 A. I. Zaitsev, A. S. Aleksandrovskii, A. V. Zamkov and A. M. Sysoev, *Inorg. Mater.*, 2006, **42**, 1360–1362.
7 L. Li, Y. Wang, B. H. Lei, S. J. Han, Z. H. Yang, K. R. Poeppelmeier and S. L. Pan, *J. Am. Chem. Soc.*, 2016, **138**, 9101–9104.
8 S. G. Zhao, P. F. Gong, S. Y. Luo, L. Bai, Z. S. Lin, Y. Y. Tang, Y. L. Zhou, M. C. Hong and J. H. Luo, *Angew. Chem., Int. Ed.*, 2015, **54**, 4217–4221.
9 S. G. Zhao, P. F. Gong, S. Y. Luo, L. Bai, Z. S. Lin, C. M. Ji, T. L. Chen, M. C. Hong and J. H. Luo, *J. Am. Chem. Soc.*, 2014, **136**, 8560–8563.
10 S. J. Clark, M. D. Segall, C. J. Pickard, P. J. Hasnip, M. J. Probert, K. Refson and M. C. Payne, *Z. Kristallogr.*, 2005, **220**, 567–570.
11 C. T. Chen, G. L. Wang, X. Y. Wang and Z. Y. Xu, *Appl. Phys. B: Lasers Opt.*, 2009, **97**, 9–25.
12 C. T. Chen, Y. B. Wang, B. C. Wu, K. C. Wu, W. L. Zeng and L. H. Yu, *Nature*, 1995, **373**, 322–324.
13 S. C. Wang, N. Ye, W. Li and D. Zhao, *J. Am. Chem. Soc.*, 2010, **132**, 8779–8786.
14 S. G. Zhao, P. F. Gong, L. Bai, X. Xu, S. Q. Zhang, Z. H. Sun, Z. S. Lin, M. C. Hong, C. T. Chen and J. H. Luo, *Nat. Commun.*, 2014, **5**, 4019.
15 H. P. Wu, S. L. Pan, K. R. Poeppelmeier, H. Y. Li, D. Z. Jia, Z. H. Chen, X. Y. Fan, Y. Yang, J. M. Rondinelli and H. S. Luo, *J. Am. Chem. Soc.*, 2011, **133**, 7786–7790.

16 S. G. Zhao, P. F. Gong, S. Y. Luo, S. J. Liu, L. Li, M. Adnan, T. Khan, M. C. Hong, Z. S. Lin and J. H. Luo, *J. Am. Chem. Soc.*, 2015, **137**, 2207–2210.
17 L. Kang, S. Luo, H. Huang, T. Zheng, Z. S. Lin and C. T. Chen, *J. Phys.: Condens. Matter*, 2012, **24**, 335503.
18 P. Yu, L. M. Wu, L. J. Zhou and L. Chen, *J. Am. Chem. Soc.*, 2014, **136**, 480–487.
19 G. E. R. Schulze, *Z. Phys. Chem., Abt. B*, 1934, **24**, 215–218.
20 Z. H. Li, Y. C. Wu, P. Z. Fu, S. L. Pan and C. T. Chen, *J. Cryst. Growth*, 2004, **270**, 486–490.
21 Z. H. Li, Z. S. Lin, Y. C. Wu, P. Z. Fu, Z. Z. Wang and C. T. Chen, *Chem. Mater.*, 2004, **16**, 2906–2908.
22 S. F. Zhang, E. P. Zhang, P. Z. Fu and Y. C. Wu, *J. Cryst. Growth*, 2009, **311**, 2433–2436.
23 G. G. Xu, J. Li, S. J. Han, Y. J. Guo and J. Y. Wang, *Kristallografiya*, 2010, **55**, 1242–1244.
24 X. Zhang, L. R. Wang, S. F. Zhang, G. L. Wang, S. G. Zhao, Y. Zhu, Y. C. Wu and C. T. Chen, *J. Opt. Soc. Am. B*, 2011, **28**, 2236–2239.
25 Z. Li, Q. Liu, S. J. Han, T. Iitaka, H. B. Su, T. Tohyama, H. D. Jiang, Y. J. Dong, B. Yang, F. F. Zhang, Z. H. Yang and S. L. Pan, *Phys. Rev. B: Condens. Matter Mater. Phys.*, 2016, **93**, 245125.
26 Z. J. Ma, K. C. Wu, R. J. Sa, K. N. Ding and Q. H. Li, *AIP Adv.*, 2012, **2**, 032170.
27 B. B. Zhang, M.-H. Lee, Z. H. Yang, Q. Jing, S. L. Pan, M. Zhang, H. P. Wu, X. Su and C.-S. Li, *Appl. Phys. Lett.*, 2015, **106**, 031906.
28 J. Li, Z. J. Ma, C. He, Q. H. Li and K. C. Wu, *J. Mater. Chem. C*, 2016, **4**, 1926–1934.
29 J. Y. Hu, Z. J. Ma, J. Li, C. He, Q. H. Li and K. C. Wu, *J. Phys. D: Appl. Phys.*, 2016, **49**, 185103.
30 L. Yang, Y. C. Yue, F. Yang and Z. Y. Xu, *Opt. Lett.*, 2016, **41**, 1598–1600.
31 J. Haines, C. Chateau, J. M. Leger and R. Marchand, *Ann. Chim. Sci. Mater.*, 2001, **26**, 209–215.
32 J. Haines, O. Cambon, R. Aster, P. Fertey and C. Chateau, *Z. Kristallogr.*, 2004, **219**, 32–38.
33 A. Baykal and A. Evren, *Turk. J. Chem.*, 2006, **30**, 723–730.
34 V. Vildosola, L. Pourovskii, R. Arita, S. Biermann and A. Georges, *Phys. Rev. B: Condens. Matter Mater. Phys.*, 2008, **78**, 064518.
35 S. J. Clark, M. D. Segall, C. J. Pickard, P. J. Hasnip, M. J. Probert, K. Refson and M. C. Payne, *Z. Kristallogr.*, 2005, **220**, 567–570.
36 B. G. Pfrommer, M. Cote, S. G. Louie and M. L. Cohen, *J. Comput. Phys.*, 1997, **131**, 233–240.
37 D. M. Ceperley and B. J. Alder, *Phys. Rev. Lett.*, 1980, **45**, 566–569.
38 J. P. Perdew and A. Zunger, *Phys. Rev. B: Condens. Matter Mater. Phys.*, 1981, **23**, 5048–5079.
39 J. P. Perdew, K. Burke and M. Ernzerhof, *Phys. Rev. Lett.*, 1996, **77**, 3865–3868.
40 J. S. Lin, A. Qteish, M. C. Payne and V. Heine, *Phys. Rev. B: Condens. Matter Mater. Phys.*, 1993, **47**, 4174–4180.
41 F. Wooten, *Optical properties of solids*, Academic, New York, 1972.
42 L. J. Sham and M. Schluter, *Phys. Rev. Lett.*, 1983, **51**, 1888–1891.
43 A. J. Cohen, P. Mori-Sanchez and W. T. Yang, *Phys. Rev. B: Condens. Matter Mater. Phys.*, 2008, **77**, 115123.
44 P. Mori-Sanchez, A. J. Cohen and W. T. Yang, *Phys. Rev. Lett.*, 2008, **100**, 146401.
45 R. He, H. W. Huang, L. Kang, W. J. Yao, X. X. Jiang, Z. S. Lin, J. G. Qin and C. T. Chen, *Appl. Phys. Lett.*, 2013, **102**, 231904.
46 A. D. Becke and E. R. Johnson, *J. Chem. Phys.*, 2006, **124**, 221101.
47 F. Tran and P. Blaha, *Phys. Rev. Lett.*, 2009, **102**, 226401.
48 P. Blaha, K. Schwarz, G. K. H. Madsen, D. Kvasnicka and J. Luitz, *WIEN2k, an Augmented Plane*.
49 D. Koller, F. Tran and P. Blaha, *Phys. Rev. B: Condens. Matter Mater. Phys.*, 2011, **83**, 195134.
50 D. Koller, F. Tran and P. Blaha, *Phys. Rev. B: Condens. Matter Mater. Phys.*, 2012, **85**, 55109.
51 M. J. Frisch, *et al.*, *Gaussian 09*, Gaussian, Wallingford, CT, 2009.
52 C. Aversa and J. E. Sipe, *Phys. Rev. B: Condens. Matter Mater. Phys.*, 1995, **52**, 14636.
53 (*a*) A. H. Reshak, V. Kityk and S. Auluck, *J. Phys. Chem. B*, 2010, **114**, 16705–16712; (*b*) I. I. Tordjman, R. Masse and J. C. Guitel, *Z. Kristallogr.*, 1974, **139**, 103–115.
54 (*a*) A. H. Reshak, H. W. Huang, H. Kamarudin and S. Auluck, *J. Appl. Phys.*, 2015, **117**, 085703; (*b*) X. S. Wang, L. J. Liu, X. Y. Wang, L. Bai and C. T. Chen, *CrystEngComm*, 2015, **17**, 925–929.